Large-scale relativistic configuration-interaction calculation of the $2s^2\,{}^1S_0-2s2p\,{}^3P_1$ intercombination transition in C III

M. H. Chen and K. T. Cheng
University of California, Lawrence Livermore National Laboratory, Livermore, California 94550

W. R. Johnson
Department of Physics, University of Notre Dame, Notre Dame, Indiana 46556

(Received 3 May 2001; published 17 September 2001)

A large-scale, relativistic configuration-interaction (RCI) method has been developed for precision calculations of transition oscillator strengths. It is based on the no-pair Hamiltonian and employs finite *B*-spline basis functions. For the $2s^2\,{}^1S_0-2s2p\,{}^3P_1$ intercombination transition in berylliumlike carbon, the present RCI expansions reach close to 200 000 configurations, and include all single and double excitations from valence-valence, core-valence, and core-core interactions, along with dominant triple and quadruple excitations. Resulting length- and velocity-gauge transition rates are very well converged, but still differ by a factor of 2. This strong gauge dependence is found to arise from the neglect of negative-energy states which has negligible effects on length-gauge results but can affect velocity-gauge results significantly. The present intercombination transition rate for C III of 101.6 ± 0.7 sec^{-1} differs from the measured value of 102.94 ± 0.14 sec^{-1} [Doerfert *et al.*, Phys. Rev. Lett. **78**, 4355 (1997)] by about 1.3%.

DOI: 10.1103/PhysRevA.64.042507 PACS number(s): 31.30.Jv, 31.25.−v, 31.10.+z, 31.15.Ar

I. INTRODUCTION

Intercombination lines are of interest in astrophysics and for plasma diagnostics. As these spin-forbidden transitions are strongly influenced by relativity and electron correlation, they can also provide stringent tests of atomic structure calculations. The $2s^2\,{}^1S_0-2s2p\,{}^3P_1$ intercombination transition in berylliumlike carbon presents a particularly interesting case. This 1909 Å line is one of the more prominent emission lines in stellar objects, and can be used for temperature and electron-density determinations, but its transition rate has not been easy to calculate accurately. Indeed, decay rates from early theoretical investigations vary widely from 70 to 130 sec^{-1} [1–8]. While some of these results are in good agreement with the ion trap measurement of 121 ± 7 sec^{-1} [9], more recent large-scale calculations based on the configuration-interaction (CIV3) [10], the multiconfiguration Hartree-Fock (MCHF) [11], and the multiconfiguration Dirac-Fock (MCDF) [12–16] methods all give results that are in the neighborhood of 100 sec^{-1} and depart from this experimental data.

The difficulty with the transition rate calculations for this intercombination line arises mainly from the strong cancellations (up to three orders of magnitude in C III) in the relativistic transition amplitudes between the $2s$-$2p_{1/2}$ and $2s$-$2p_{3/2}$ matrix elements in the LS-coupling limit. As a result, even small contributions from residual electron correlations and higher-order relativistic corrections become very important. For example, while some early calculations did not include the Breit interaction, it has been shown to reduce the transition rate by over 30% in C III [13], which is unusually large for such low-Z ion. Also, in MCDF calculations, some configuration expansions can lead to MCDF equations for orbital optimizations that do not reduce to the correct nonrelativistic limit. Ordinarily, this is not a serious problem, but in this case, transition rates can be affected by a factor of 3 in C III if this problem is left untreated [12]. Furthermore, instead of being restricted to a common set of basis orbitals, initial and final states were independently optimized in MCDF calculations [12,15], leading to nonorthogonal sets of basis functions. Once again, these normally small orbital overlap corrections cannot be ignored, and must be handled correctly. These and other problems make precision calculations of this transition rate very difficult. However, with steady improvements in theory, results are showing signs of convergence at the level of a few percent.

Recently, a high-precision heavy-ion storage ring measurement [17] yielded a result of 102.94 ± 0.14 sec^{-1} which agrees very well with the latest large-scale MCDF calculation of 102.9 ± 1.5 sec^{-1} [15]. In spite of such good agreement, however, there are unresolved issues in theory. To begin with, at the 1% level, the importance of small corrections such as those from core-core excitations and retarded Breit interactions have not been thoroughly investigated. What is more important, even though these MCDF results appear to be very well converged, there remains a large discrepancy, up to 60%, between the length- and velocity-gauge transition rates [15]. While velocity-gauge results are expected to converge much more slowly than length-gauge results, such a strong gauge dependence is still puzzling. Apparently, even after all these theoretical efforts, much work remains to be done for a better understanding of this intercombination line.

To this end, we have developed a large-scale, relativistic configuration-interaction (RCI) method for precision calculations of transition oscillator strengths, and apply it here to study the $2s^2\,{}^1S_0-2s2p\,{}^3P_1$ spin-forbidden transition in C III. Relativistic and correlation effects are systematically considered to ensure the convergence of our results. Calculations are also carried out for the $2s^2\,{}^1S_0-2s2p\,{}^1P_1$ spin-allowed transition, and comparisons between these two results clearly show the enhanced effects of small corrections such as the Breit interaction on the spin-forbidden transition. Perhaps the most intriguing manifestation of these enhanced

effects is in the gauge invariance of these results: While the length- and velocity-gauge transition rates are in very good agreement for the $^1P_1$ transition, they disagree by a factor of 2 for the $^3P_1$ transition even though our RCI results are very well converged. With the aid of analyses based on the relativistic many-body perturbation theory (RMBPT) [18–20], we shall show that this strong gauge dependence is due to the neglect of negative-energy states which have essentially no effect on the $^1P_1$ transition nor on the length-gauge results, but can affect the velocity-gauge results of the $^3P_1$ transition significantly.

II. THEORETICAL METHOD

Details of our RCI method for structure calculations were presented before [21,22]. Briefly, RCI is based on the no-pair Hamiltonian [23–25] which includes the Coulomb and frequency-dependent retarded Breit interactions. One-electron *B*-spline basis functions are obtained by solving the Dirac equation of an electron moving in a Coulomb or model potential confined in a cavity [26]. Typically, the first 20–24 out of 30 positive-energy *B*-spline orbitals generated for each of the *s*, *p*, *d*, ..., symmetries are used in our RCI calculations, and the same basis set is used for both the initial and final states. The advantage of using these *B*-spline orbitals is that they provide a complete description of correlation contributions from the bound and continuum states. Also, orthonormality and nonrelativistic limits are strictly satisfied. The trade-off for not using more optimized basis functions, however, is that we must deal with rather large basis sets typically consisting of 200–300 orbitals. We use Davidson's method [27] (also see Ref. [28]) to solve the resulting large-scale eigenvalue problems for the initial and final states. These are computer intensive calculations which can run for days on fast computers and need many gigabytes of temporary disk space to store the large, sparse RCI matrices. The computing efficiency and disk space management algorithms of our codes have been greatly improved to allow for very large-scale calculations.

In this work, radiative transition rates are calculated from first-order perturbation theory using the frequency-dependent electromagnetic multipole transition operator in both length and velocity gauges [18,29] for the $2s^2\,{}^1S_0$–$2s2p\,{}^{1,3}P_1$ transitions in berylliumlike carbon. (Note that the velocity gauge is the same as the Coulomb gauge.) Angular recoupling coefficients used in the present transition rate calculations are computed with the MCT package [30] which is consistent with the MCP [30] angular recoupling package used in our energy-level calculations. The most time-consuming part of these large-scale transition rate calculations is in the evaluation of millions and millions of angular recoupling coefficients which are largely independent of the principal quantum numbers *n* of the basis functions. As in our structure calculations [21,22], we use an angular channel scheme to speed up these calculations. In this scheme, we only need to evaluate a few thousand angular coefficients for the distinct angular channels. Resulting calculations are still time consuming, but are not nearly as computer intensive as the structure part of these calculations.

Our RCI expansions consist of configuration-state functions (CSF's) that arise from multiple excitations from the reference configurations $1s^22s^2+1s^22p^2$ for the $^1S_0$ ground state and $1s^22s2p$ for the $^{1,3}P_1$ excited states. To systematically study the effects of single and double (SD) excitations, we begin by including the $1s^2nln'l'$ CSF's that arise from the excitations of one or two valence electrons to account for the valence-valence (VV) interactions. We then add the $1s2snln'l'$ and $1s2pnln'l'$ CSF's which arise from one electron excited from the $1s^2$ core with or without another electron excited from the valence shells. Changes in the transition energies and rates give the core-valence (CV) contributions. Finally, two-electron excitations from the core are included to account for the core-core (CC) interactions. These additional CSF's consist of $2s^2nln'l'$ and $2p^2nln'l'$ for the $^1S_0$ state and $2s2pnln'l'$ for the $^{1,3}P_1$ states. With n, $n'\leqslant 22$ and l, $l'\leqslant 5$, our RCI expansions include up to 56 562 CSF's for the ground state and 139 585 CSF's for the excited states based on SD excitations from the reference configurations. Contributions from higher partial waves with $l>5$ are small and are obtained by extrapolations.

Contributions from triple and quadruple (TQ) excitations are calculated separately. The basic CSF's considered here are $1s3snln'l'$, $1s3pnln'l'$, and $1s3dnln'l'$. Additional CSF's from other dominant TQ excitations include $2s3snln'l'$, $2p3pnln'l'$, $3s^2nln'l'$, $3p^2nln'l'$, and $3d^2nln'l'$ for the $^1S_0$ state and $2s3pnln'l'$, $2p3snln'l'$, $2p3dnln'l'$, $3s3pnln'l'$, and $3p3dnln'l'$ for the $^{1,3}P_1$ states. With n, $n'\leqslant 20$ and l, $l'\leqslant 2$, total numbers of CSF's including SD and TQ excitations amount to 64 252 for the ground state and 197 426 for the excited states. Differences with corresponding calculations with SD excitations only give the TQ contributions. These are small corrections and residual contributions from $n>20$ and $l>2$ are found to be quite negligible.

In principle, our RCI transition energies and rates should be independent of the model potential used to generate the *B*-spline basis functions. To test the convergence of our results, we perform the calculations in two different model potentials: the four-electron Dirac-Kohn-Sham (DKS) potential and the three-electron modified core-Hartree (MCH) potential. The DKS potential is the Dirac-Slater potential of the $1s^22s^2$ berylliumlike ground state with the Kohn-Sham exchange approximation, while the MCH potential is the Dirac-Hartree potential of the $1s^22s$ lithiumlike ground state with no exchange interaction. It should be noted that individual VV, CV, CC, and TQ contributions are still potential dependent, and more appropriate choices of model potentials like the DKS instead of, for example, the bare nuclear Coulomb potential, can minimize contributions from residual correlation corrections and speed up the convergence of RCI results. Also note that with the neglect of negative-energy states by the no-pair Hamiltonian, RCI transition energies are known to be slightly potential dependent [31], even though this effect is generally very small and is expected to be completely negligible for low-Z ions like C III.

III. RESULTS AND DISCUSSION

Contributions from VV, CV, and CC interactions to the $2s^2\,{}^1S_0$–$2s2p\,{}^{1,3}P_1$ transition energies in C III are listed in

TABLE I. Transition energies (cm^{-1}) for the $^1S_0$- $^3P_1$ and $^1S_0$- $^1P_1$ transitions in C III.

		$^1S_0$- $^3P_1$				$^1S_0$- $^1P_1$			
Type	Contribution	VV	CV	CC	Sum	VV	CV	CC	Sum
DKS	Coulomb	52 685	−113	−146	52 426	103 117	−443	−2	102 672
	$B(\omega=0)$	2	3	−1	4	−7	1	3	−3
	$B(\omega\neq 0)$	0	0	0	0	0	0	0	0
	l-extrap	0	0	0	0	−52	−2	−1	−55
	SD	52 687	−110	−147	52 430	103 058	−444	0	102 614
	TQ				−11				−71
	QED+MP [a]				−24				−24
	Total				52 395				102 519
MCH	Coulomb	54 553	−2007	−124	52 422	104 482	−1788	−20	102 674
	$B(\omega=0)$	5	0	−1	4	−11	7	1	−3
	$B(\omega\neq 0)$	0	0	0	0	0	0	0	0
	l-extrap	0	0	0	0	−52	−5	0	−57
	SD	54 558	−2007	−125	52 426	104 419	−1786	−19	102 614
	TQ				−11				−89
	QED+MP [a]				−24				−24
	Total				52 391				102 501
Expt. [b]					52 391				102 352

[a]Reference [15].
[b]NIST online database.

Table I, along with corrections from high-l extrapolations and TQ excitations. Also listed here are contributions from QED and mass polarization (MP) corrections from Ref. [15]. For such a low-Z ion, the effects of unretarded Breit interaction $B(\omega=0)$ on these transition energies are small, and the retarded part of Breit corrections $B(\omega\neq 0)$ are completely negligible. Our $^1S_0$–$^3P_1$ transition energy converges very rapidly, and is in very good agreement with experiment. The $^1P_1$ excited state, on the other hand, is known to converge more slowly [22], as is evident from the relatively large corrections from high-l extrapolations and TQ excitations to the $^1S_0$-$^1P_1$ transition energy which has a residual discrepancy with experiment of about 160 cm^{-1}.

In Table II, our RCI results on the oscillator strengths of the $2s^2\,^1S_0$–$2s2p\,^1P_1$ transition in C III are shown. In our transition calculations, high-l extrapolations are performed on transition matrix elements only to give the ''l-extrap'' contributions. As found for transition energies, contributions from the Breit interaction are very small. Also, correlation corrections from CV, CC, and TQ excitations are, in general, not very significant and VV results alone are already accurate to about 2%. The only exception is the velocity-gauge MCH results where the CV corrections can be as much as 20%. This clearly shows that intermediate results can still be potential dependent, and underscores the importance of using more appropriate model potentials or better optimized basis functions in small-scale RCI calculations.

At each of the intermediate steps, oscillator strengths are calculated with corresponding intermediate-step theoretical transition energies which may not be very accurate. We have replaced all theoretical energies with the empirical energy, and recalculated the oscillator strengths. This affects our results directly through the transition energy multiplicative factor to the line strengths, as well as indirectly through the frequency-dependent Bessel functions in the transition matrix elements. The ''direct'' corrections are the most common form of empirical energy corrections which scale the length- and velocity-gauge oscillator strengths by the same factor of $\xi=E_{\text{empirical}}/E_{\text{theory}}$. The ''indirect'' corrections, on the other hand, can affect the length- and velocity-gauge transition amplitudes differently, and actually play a crucial role in preserving the gauge invariance of this transition.

As shown in Table II, before empirical energy corrections are made, length- and velocity-gauge results converge to values that differ by about 0.7%. These corrections reduce the length-gauge results by 0.3%, which are consistent with changes made by the direct energy scalings, but increase the velocity-gauge results by 0.4% which can only be caused by the indirect changes to the transition amplitudes. Indeed, while the length-gauge amplitude is insensitive to energy corrections because its leading ω/c expansion term is the usual dipole matrix element

$$\int dr\, r(P_iP_f+Q_iQ_f),$$

which is frequency independent, the velocity-gauge amplitude is sensitive to energy corrections because its leading ω/c expansion term is

$$\frac{c}{\omega}\int dr[P_iQ_f(\kappa_f-\kappa_i+1)+Q_iP_f(\kappa_f-\kappa_i-1)],$$

which is frequency dependent. This also means that the oscillator strength is roughly proportional to the transition en-

TABLE II. Length- and velocity-gauge oscillator strengths for the $2s^2\,{}^1S_0$–$2s2p\,{}^1P_1$ transition in C III.

		Length				Velocity			
Type	Contribution	VV	CV	CC	Sum	VV	CV	CC	Sum
DKS	Coulomb	0.7716	−0.0116	−0.0006	0.7594	0.7714	−0.0150	−0.0041	0.7523
	$B(\omega=0)$	0.0001	0.0000	0.0000	0.0001	0.0004	−0.0005	0.0000	−0.0001
	$B(\omega\neq 0)$	0.0000	0.0000	0.0000	0.0000	0.0000	0.0000	0.0000	0.0000
	l-extrap	0.0003	−0.0002	0.0000	0.0001	−0.0004	−0.0001	0.0000	−0.0005
	SD	0.7720	−0.0118	−0.0006	0.7596	0.7714	−0.0156	−0.0041	0.7517
	TQ				0.0005				0.0032
	Total				0.7601				0.7549
	E-adjust				0.7577				0.7578
	Neg-E				0.7577				0.7578
MCH	Coulomb	0.7772	−0.0173	0.0003	0.7602	0.5993	0.1564	−0.0026	0.7531
	$B(\omega=0)$	0.0000	0.0001	0.0000	0.0001	0.0004	−0.0005	0.0000	−0.0001
	$B(\omega\neq 0)$	0.0000	0.0000	0.0000	0.0000	0.0000	0.0000	0.0000	0.0000
	l-extrap	0.0003	−0.0002	−0.0001	0.0000	−0.0004	−0.0001	0.0000	−0.0005
	SD	0.7775	−0.0174	0.0002	0.7603	0.5993	0.1558	−0.0026	0.7525
	TQ				0.0001				0.0029
	Total				0.7604				0.7554
	E-adjust				0.7579				0.7579
	Neg-E				0.7579				0.7579

ergy in the length gauge, but inversely proportional to the transition energy in the velocity gauge. As a result, leading empirical energy corrections can be obtained simply by scaling the length- and velocity-gauge results with the factors ξ and $1/\xi$, respectively. The actual -0.3% and $+0.4\%$ corrections shown here are clearly consistent with these scaling approximations.

The fact that the resulting ''E-adjust'' oscillator strengths are nearly gauge independent is not a coincidence. As pointed out in Ref. [20], gauge invariance can be preserved order by order in RMBPT only by including the derivative terms of the frequency-dependent transition matrix elements which arise from changes in the transition energy from previous orders of perturbation corrections. Essentially, ''indirect'' empirical energy corrections are numerical manifestations of these derivative terms in RCI calculations. Indeed, similar improvements in the gauge independence of this transition rate by empirical energy corrections were also observed in the recent MCDF calculation [15].

Also shown in Table II are final results labeled as ''Neg-E'' after contributions from the negative-energy states are included. We shall postpone the discussions of these corrections until later. For the $^1S_0-{}^1P_1$ transition, the effects of negative-energy states are negligible, and final results are seen to be quite potential and gauge independent.

In Table III, our RCI results on the decay rates of the $2s^2\,{}^1S_0$–$2s2p\,{}^3P_1$ transition in C III are shown. As mentioned earlier, strong cancellations between the $2s$-$2p_{1/2}$ and $2s$-$2p_{3/2}$ matrix elements suppress the transition amplitudes by over three orders of magnitudes here, leading to transition rates of about 1.0×10^2 sec^{-1} for this spin-forbidden transition, as compared to 1.764×10^9 sec^{-1} for the $^1S_0$-$^1P_1$ spin-allowed transition. As a result, small corrections which are otherwise quite negligible can become very important. This is evident in the unusually strong effects of Breit interaction which reduce the length-gauge transition rates by 26% and increase the velocity-gauge results by 50%. However, the frequency-dependent part of the Breit interaction only reduces the length-gauge transition rates by 0.03 sec^{-1}, which is much smaller than the estimate of 2 sec^{-1} given in the recent MCDF calculation [15]. While these transition rates are dominated by contributions from low partial waves, contributions from high partial waves with $l>5$ are not negligible. They are obtained by extrapolations using a $1/l^4$ scaling rule and amount to 0.5% to 1% corrections.

Electron correlations play a key role in precision calculations of the transition rate for this intercombination line. In Table III, it can be seen that CV interactions increase the length-gauge decay rate calculated in the DKS potential by 7% from 97.74 to 104.82 sec^{-1}, while they reduce corresponding MCH decay rate by 13% from 119.83 to 104.23 sec^{-1}. This improves the agreement between the two potential results from 23% to 0.6%. CC interactions further reduce these rates by 3% to 101.30 and 101.57 sec^{-1} for the DKS and MCH potentials, respectively, and the agreement between these two length-gauge decay rates from all SD excitations improves to 0.3%. This potential dependence is further reduced to 0.2% with the inclusion of TQ corrections, which increase the decay rates slightly by about 0.5%. Finally, empirical energy corrections are small and amount to 0.2% rate reductions only.

Electron correlations play an even more important role for the velocity-gauge transition rates. For the DKS potential, CV and CC corrections change the VV result of 112.44 sec^{-1} to the full SD excitation result of 192.90 sec^{-1} for an increase of about 70%, while the cor-

TABLE III. Length- and velocity-gauge transition rates (sec^{-1}) for the $2s^2\ ^1S_0$–$2s2p\ ^3P_1$ transition in C III.

		Length				Velocity			
Type	Contribution	VV	CV	CC	Sum	VV	CV	CC	Sum
DKS	Coulomb	134.06	5.40	−2.55	136.91	132.01	0.72	−5.56	127.17
	$B(\omega=0)$	−36.72	1.61	−1.04	−36.15	−20.04	87.12	−3.02	64.06
	$B(\omega\neq0)$	−0.03	0.00	0.00	−0.03	−0.09	−0.03	0.01	−0.11
	l-extrap	0.43	0.07	0.07	0.57	0.56	0.27	0.95	1.78
	SD	97.74	7.08	−3.52	101.30	112.44	88.08	−7.62	192.90
	TQ				0.50				1.61
	Total				101.80				194.51
	E-adjust				101.57				193.40
	Neg-*E*				101.57				100.88
MCH	Coulomb	163.95	−25.28	−1.45	137.22	67.74	62.00	−2.81	126.93
	$B(\omega=0)$	−44.59	9.68	−1.24	−36.15	−3.21	66.74	−0.22	63.31
	$B(\omega\neq0)$	0.00	−0.03	0.00	−0.03	−0.05	−0.04	0.00	−0.09
	l-extrap	0.47	0.03	0.07	0.57	0.38	0.43	−0.02	0.79
	SD	119.83	−15.60	−2.62	101.61	64.86	129.13	−3.05	190.94
	TQ				0.42				1.37
	Total				102.03				192.31
	E-adjust				101.83				191.92
	Neg-*E*				101.83				108.18

responding increase in the MCH decay rate is close to a factor of 3, from 64.86 to 190.94 sec^{-1}. TQ corrections for the velocity-gauge results, at about 1.5 sec^{-1}, are also larger than those for the length-gauge results by a factor of 3. Even empirical energy adjustments are much more significant here. Resulting velocity-gauge transition rates of 194.51 and 192.31 sec^{-1} for the two potentials agree to about 1%, a marked improvement over the two VV results, which differ by almost a factor of 2.

Our final "*E*-adjust" intercombination transition rates as calculated in the length and velocity gauges are 101.6 ± 0.7 and 193.4 ± 2.0 sec^{-1}, respectively, for the DKS potential and 101.8 ± 0.7 and 191.9 ± 2.0 sec^{-1}, respectively, for the MCH potential. Theoretical uncertainties are assigned by taking into account the potential dependence of the results, possible errors in high-*l* extrapolations, estimations of residual, uncalculated TQ contributions, and sensitivities to basis set selections. But while our RCI length- and velocity-gauge results agree to within 0.006% for the $^1P_1$ transition, they differ by almost a factor of 2 here. This large disparity cannot be explained by residual correlation effects in view of the level of convergence that our RCI results have achieved.

IV. NEGATIVE-ENERGY STATE CONTRIBUTIONS

The problem can be traced to the neglect of negative-energy states in our RCI calculations. Specifically, starting from second-order perturbation calculations, negative-energy states show up *explicitly* in transition matrix elements that contain sums over intermediate states but their contributions are excluded from calculations based on the no-pair Hamiltonian. The fact that length- and velocity-gauge transition rates can be different in such RMBPT and RCI calculations was discussed for heliumlike ions before [18,19], and rules for obtaining transition amplitudes that preserve the gauge invariance in RMBPT were given in Ref. [20]. In this work, we use the gauge-invariant, second-order RMBPT to investigate the effect of negative-energy states on the $^1S_0$-$^3P_1$ transition in C III.

In Fig. 1, length- and velocity-gauge transition rates for this intercombination line are shown as functions of the x_α parameter in Dirac-Slater-like potentials used to generate the one-electron *B*-spline basis functions for these RMBPT calculations. The x_α parameter is an adjustable multiplier that

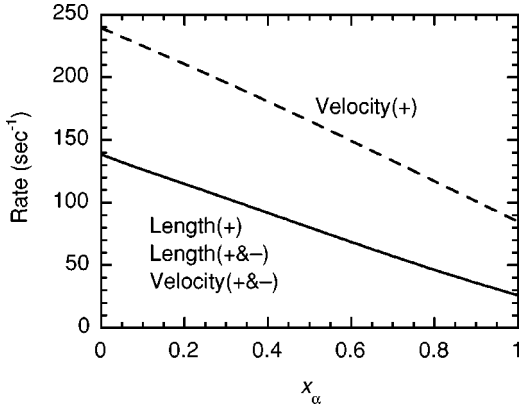

FIG. 1. Second-order RMBPT intercombination transition rates for C III as functions of the x_α parameter. The dashed line represents velocity-gauge results calculated with positive-energy states only. The solid line represents similar length-gauge results, as well as length- and velocity-gauge results calculated with both positive- and negative-energy states.

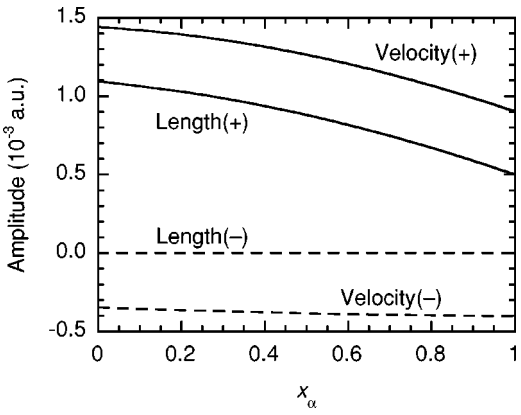

FIG. 2. Second-order RMBPT intercombination transition amplitudes for C III as functions of the x_α parameter. Solid lines are positive-energy results. Dashed lines are negative-energy results.

modifies the Slater-exchange potentials. In particular, $x_\alpha=0$ gives the Dirac-Hartree potential without exchanges, $x_\alpha=2/3$ is the Dirac-Kohn-Sham potential used in our RCI calculations, and $x_\alpha=1$ is the full Dirac-Slater potential. Contrary to the RCI results, second-order RMBPT transition rates are not very well converged and are strongly potential dependent. Indeed, length-gauge transition rates vary from 140 sec^{-1} at $x_\alpha=0$ to 26 sec^{-1} at $x_\alpha=1$. Without negative-energy states, RMBPT velocity-gauge results are consistently larger than the length-gauge results by about a factor of 2, just like the RCI results. With negative-energy states, however, length-gauge results remain the same while velocity-gauge results are greatly reduced, resulting in complete agreement between the two gauges, as they should be order-by-order in perturbation theory.

In Fig. 2, positive- and negative-energy RMBPT transition amplitudes are shown as functions of the x_α parameter. As shown in the figure, negative-energy amplitudes are essentially zero in the length gauge, but are consistently very large in the velocity gauge. However, these velocity-gauge amplitudes do not vary nearly as rapidly with the x_α parameter as their positive-energy counterparts, indicating that they may be reasonably well converged and can be used to correct the RCI velocity-gauge results.

Indeed, adding these negative-energy transition amplitudes taken at $x_\alpha=2/3$ to the RCI transition amplitudes calculated in the same DKS potential changes the RCI velocity-gauge result from 193.40 to 100.88 sec^{-1}, which agrees with the RCI length-gauge result of 101.57 sec^{-1} to within 0.7%. Likewise, correcting the RCI velocity-gauge result obtained in the MCH potential with RMBPT negative-energy amplitudes calculated in the same potential changes the RCI result from 191.92 to 108.18 sec^{-1} which is also in much better agreement with the MCH length-gauge result of 101.83 sec^{-1}. These negative-energy corrected RCI results are shown as "Neg-E" in Tables II and III. Negative-energy states have essentially no effects on the $^1S_0-{}^1P_1$ spin-allowed transition.

V. CONCLUSIONS

In Table IV, we compare our length-gauge $^1S_0$-$^1P_1$ oscillator strength and $^1S_0$-$^3P_1$ transition rate as calculated in the DKS potential with other theories and with experiment. For the $^1P_1$ transition, most theories are consistent with each other and with experiment. In particular, our RCI is in excellent agreement with the recent large-scale MCDF calculation

TABLE IV. Comparisons between theory and experiment on the decay rates $A(\text{sec}^{-1})$ of the $2s^2\,{}^1S_0-2s2p\,{}^3P_1$ spin-forbidden transition and the oscillator strengths gf of the $2s^2\,{}^1S_0-2s2p\,{}^1P_1$ spin-allowed transition in C III.

Method	$A(^3P_1)$	$gf(^1P_1)$	Reference	Year
CI	77	0.708 [a]	[1]	1972
RRPA	110	0.753	[2]	1977
CI+Breit	86(9)		[3]	1978
Model potential	110(16)	0.764	[4]	1978
CI	96(11)	0.768 [a]	[5]	1978
MCDF	79	0.794	[6]	1979
MCRRPA	118	0.791	[7]	1994
MZ	120		[8]	1995
CIV3	104(4) [b]	0.7587	[10]	1994
MCHF	103(3)	0.7566(20)	[11]	1994
MCDF	100.1 [c]		[12]	1998
MCDF+RCI	100.3(40)	0.7571(20)	[13]	1995
MCDF+RCI	103.0(4)	0.7563(20)	[14]	1997
MCDF+RCI	102.9(15)	0.7579(4)	[15]	1998
Present work	101.6(7)	0.7577(3)		2001
Experiment	102.94(14)	0.754(14)	[17,32]	1997,1986

[a]Converted from the decay rate with the empirical transition energy.

[b]With empirical transition energy, $^1P_1$-$^3P_1$ separation, and ^3P fine-structure corrections.

[c]With nonrelativistic limit and nonorthogonal basis set corrections.

[15]. For the $^3P_1$ transition, early theoretical results varied widely and were highly uncertain, but recent large-scale calculations generally agree with experiment to within a few percent. However, some of these theoretical data include empirical energy corrections which can be quite substantial. In the case of CIV3 [10], for example, empirical values of the transition energy, the $^1P_1-^3P_1$ level separation, and the $^3P_{0,1,2}$ fine-structure splittings have all been used to change the transition rate from the *ab initio* value of 98 sec^{-1} to the corrected value of 104 sec^{-1} shown in Table IV. While empirical corrections are also made in the present RCI calculation, they involve the transition energy only, and change the length-gauge results by merely 0.2%, which are well within the estimated theoretical uncertainty. Our RCI $^3P_1$ transition rate again agree very well with the large-scale MCDF calculation [15] but is slightly outside the error bar of the recent high-precision storage ring measurement [17].

In this work, we have carried out systematic studies of the relativistic and correlation contributions to the $2s^2\,{}^1S_0-2s2p\,{}^{1,3}P_1$ transitions in C III with our large-scale RCI method. For the $^1P_1$ spin-allowed transition, we have shown that empirical energy corrections to the frequency-dependent transition matrix elements, though small in size, play a crucial role in preserving the gauge invariance. As for the $^3P_1$ spin-forbidden transition, length- and velocity-gauge transition rates are found to converge to values that differ by almost a factor of 2 and, contrary to common beliefs, this discrepancy is simply too large to be explained by residual correlation effects. With analyses based on the RMBPT, we have also shown that the gauge invariance of this intercombination transition can be preserved only by including contributions from the negative-energy states in velocity-gauge calculations. Since negative-energy states are excluded by the no-pair Hamiltonian, length- and velocity-gauge RCI results will always be different for this $^3P_1$ transition and length-gauge results, which are unaffected by the negative-energy states, appear to be more reliable and should be used. This is also true for other relativistic calculations (such as MCDF) where negative-energy states are not *explicitly* considered. The present intercombination transition rate in C III of 101.6 ± 0.7 sec^{-1} is very well converged but still differs from the measured value of 102.94 ± 0.14 sec^{-1} [17] by 1.3%. More precision measurements of this intercombination transition in C III, as well as in nearby berylliumlike ions, are highly desirable.

ACKNOWLEDGMENTS

The work of M.H.C. and K.T.C. was performed under the auspices of the U.S. Department of Energy by the University of California, Lawrence Livermore National Laboratory under Contract No. W-7405-Eng-48. The work of W.R.J. was supported in part by NSF Grant No. Phy 99-70666.

[1] H. Nussbaumer, Astron. Astrophys. **16**, 77 (1972).
[2] C.D. Lin and W.R. Johnson, Phys. Rev. A **15**, 1046 (1977).
[3] R. Glass and A. Hibbert, J. Phys. B **11**, 2413 (1978).
[4] C. Laughlin, E.R. Constantinides, and G.A. Victor, J. Phys. B **11**, 2243 (1978).
[5] H. Nussbaumer and P.J. Storey, Astron. Astrophys. **64**, 139 (1978).
[6] K.T. Cheng, Y.K. Kim, and J.P. Desclaux, At. Data Nucl. Data Tables **24**, 111 (1979).
[7] H.S. Chou, H.-S. Chi, and K.-N. Huang, Chin. J. Phys. (Taipei) **32**, 261 (1994).
[8] Y.V. Ralchenko and L.A. Vainstein, Phys. Rev. A **52**, 2449 (1995).
[9] V.H.S. Kwong, Z. Fang, T.T. Gibbons, W.H. Parkinson, and P.L. Smith, Astrophys. J. **411**, 431 (1993).
[10] J. Fleming, A. Hibbert, and R.P. Stafford, Phys. Scr. **49**, 316 (1994).
[11] C. Froese Fischer, Phys. Scr. **49**, 323 (1994).
[12] Y.K. Kim, F. Parente, J.P. Marques, P. Indelicato, and J.P. Desclaux, Phys. Rev. A **58**, 1885 (1998).
[13] A. Ynnerman and C. Froese Fischer, Phys. Rev. A **51**, 2020 (1995).
[14] C. Froese Fischer and G. Gaigalas, Phys. Scr. **56**, 436 (1997).
[15] P. Jönsson and C. Froese Fischer, Phys. Rev. A **57**, 4967 (1998).
[16] P. Jönsson, C. Froese Fischer, and E. Träbert, J. Phys. B **31**, 3497 (1998).
[17] J. Doerfert, E. Träbert, A. Wolf, D. Schwalm, and O. Uwira, Phys. Rev. Lett. **78**, 4355 (1997).
[18] W. R. Johnson, D. R. Plante, and J. Sapirstein, in *Advances in Atomic, Molecular, and Optical Physics*, edited by B. Bederson and H. Walther (Academic Press, San Diego, 1995), p. 251.
[19] A. Derevianko, I.M. Savukov, W.R. Johnson, and D.R. Plante, Phys. Rev. A **58**, 4453 (1998).
[20] I.M. Savukov and W.R. Johnson, Phys. Rev. A **62**, 052506 (2000).
[21] M.H. Chen, K.T. Cheng, W.R. Johnson, and J. Sapirstein, Phys. Rev. A **52**, 266 (1995).
[22] M.H. Chen and K.T. Cheng, Phys. Rev. A **55**, 166 (1997).
[23] G.E. Brown and D.G. Ravenhall, Proc. R. Soc. London, Ser. A **208**, 552 (1951).
[24] J. Sucher, Phys. Rev. A **22**, 348 (1980).
[25] M.H. Mittleman, Phys. Rev. A **4**, 893 (1971); **5**, 2395 (1972); **24**, 1167 (1981).
[26] W.R. Johnson, S.A. Blundell, and J. Sapirstein, Phys. Rev. A **37**, 307 (1988).
[27] E.R. Davidson, J. Comput. Phys. **17**, 87 (1975).
[28] A. Stathopoulos and C. Froese Fischer, Comput. Phys. Commun. **79**, 268 (1994).
[29] I.P. Grant, J. Phys. B **7**, 1458 (1974).
[30] I.P. Grant, B.J. McKenzie, P.H. Norrington, D.F. Mayers, and N.C. Pyper, Comput. Phys. Commun. **21**, 207 (1980).
[31] J. Sapirstein, K.T. Cheng, and M.H. Chen, Phys. Rev. A **59**, 259 (1999).
[32] N. Reistad and I. Martinson, Phys. Rev. A **34**, 2632 (1986).